

# The segregation of poly(styrene-*b*-isoprene) diblock copolymers to the surface of a polystyrene melt: the effect of the ratio of block lengths

K. Kunz<sup>1,a</sup>, S.H. Anastasiadis<sup>1,b,c</sup>, M. Stamm<sup>2</sup>, T. Schurrat<sup>3</sup>, and F. Rauch<sup>3</sup>

<sup>1</sup> Foundation for Research and Technology - Hellas, Institute of Electronic Structure and Laser,  
P.O. Box 1527, 711 10 Heraklion Crete, Greece

<sup>2</sup> Max-Planck-Institut für Polymerforschung, Postfach 3148, 55021 Mainz, Germany

<sup>3</sup> Universität Frankfurt, Institut für Kernphysik, 60486 Frankfurt am Main, Germany

Received: 20 July 1998 / Received in final form and Accepted: 11 September 1998

**Abstract.** The effect of the ratio of block lengths on the interfacial partitioning of poly(styrene-block-1,4 isoprene) diblock copolymers from their mixtures with polystyrene homopolymer melt is investigated utilizing a series of copolymers with almost constant molecular weight but different compositions. The concentration profile of the copolymer is measured directly using the <sup>15</sup>N nuclear reaction analysis technique; a segregation of the diblock is found at both the air/polymer surface, due to the lower surface energy of polyisoprene, and at the substrate/polymer interface. No significant effect of the block length ratio on the free-surface excess was observed. The block molecular weights have apparently led to dangling chain conformations in the non-overlapping mushroom and in the overlapping mushroom regimes whereas the brush regime was not accessible; no indications of a real border between the two former regimes was found.

**PACS.** 68.10.Gw Interface activity, spreading – 68.10.m Fluid surfaces and fluid-fluid interfaces – 68.55.a Thin film structure and morphology

## 1 Introduction

The structure and composition of the near surface and/or interface regions in multicomponent polymeric systems control important properties like wetting and adhesion, and, in that respect, the applications of such systems. In the case of these multiconstituent films, segregation of components to either the air/polymer or/and the polymer/substrate interfaces determine the applicability of these materials in the coatings area.

Block copolymers consisting of two chemically different chains connected at one of their ends have been known to exhibit surfactant-like behavior, thus modifying surface/interfacial tension, adhesion, friction and wear properties. The partitioning of block copolymers (BCP) to surfaces has been of growing interest in the past years, and there have been a number of investigations, especially on the adsorption of block copolymers from solution (see, *e.g.*, Refs [1–10]). In contrast, there have been relatively few studies of surface anchored

layers formed by either block copolymer segregation from copolymer/homopolymer mixtures to a free and/or substrate interface [11–14] and to a polymer/polymer interface [15–19], or by interfacial partitioning of an end-functionalized homopolymer from a homopolymer mixture [20–22]. The situation in the melt may, in principle, be similar to the adsorption from solution; however, the polymeric nature of the “solvent” molecules should influence the behavior [23–30].

For block copolymers mixed with a homopolymer, surface segregation takes place similarly to the case of homopolymer blends. In the case of an AB diblock copolymer with an A block, which exhibits a lower surface energy and interacts unfavorably with the matrix homopolymer, and a B block compatible with the homopolymer, the A block acts as an anchor to the surface or the substrate whereas the B block dangles into the matrix. The conformation of the dangling block depends on the grafting density (influenced by the size of the anchoring block) as well as on the ratio of the size of the dangling block to that of the polymeric “solvent”. The case of end-anchored chains has mostly attracted the attention of theoreticians, with two “classical” limiting regimes discussed [23,31]. In the mushroom regime (for low grafting densities) the dangling chains do not overlap and their conformation is not disturbed; one can

<sup>a</sup> Present address: Max-Planck-Institut für Polymerforschung, Postfach 3148, 55021 Mainz, Germany.

<sup>b</sup> e-mail: spiros@iesl.forth.gr

<sup>c</sup> Also at University of Crete, Physics Department, 710 03 Heraklion Crete, Greece.

find the same scaling for the radius of gyration as in the bulk. In the brush regime (for high grafting densities) at the other limit the dangling chains are stretched [31]; two sub-regimes are discussed (wet and dry brush) depending on the penetration of the matrix homopolymer into the brush [23,24,27–30]. The region between the non-overlapping mushroom and the brush configurations has been recently discussed [27–30] in detail with various sub-regimes having been identified. For “solvent” molecular weight ( $P$  segments) larger than that of the dangling chains ( $N$  segments), the intermediate region is simpler and partially overlapping mushrooms are envisioned without any significant chain stretching; the conformation of the grafted chain is still expected to be Gaussian. Therefore, for  $P > N$ , three regimes are envisioned: non-overlapping mushrooms for  $\sigma a^2 < N^{-1}$ ; overlapping mushrooms for  $N^{-1} < \sigma a^2 < N^{-1/2}$ ; dry brush for  $\sigma a^2 > N^{-1/2}$ . Here,  $\sigma$  is the surface density of anchored chains and  $a$  the statistical segment length. For the adsorption of diblock copolymers from solution, it was shown both theoretically [4] and experimentally [9,10] that the mushroom or brush configuration is influenced by the ratio of the two block lengths with a maximum in the adsorbed amount expected for a certain ratio of the block lengths. Note that, for end-grafted chains in solution, the transition from mushrooms to brushes as a function of grafting density is estimated to be very broad [2].

The investigations performed so far on surface segregation of block copolymers in the melt are different from that presented here since they were focused on demonstrating the interfacial segregation and investigating the dependence of the adsorbed amount on bulk volume fraction essentially in the brush regime [11–13] or on the surface enrichment occurred *via* segregation of micelles [14]. In this study we investigate the effect of a variation of the ratio of the block lengths on the interfacial segregation of poly(styrene-*b*-isoprene) diblock copolymers in a polystyrene matrix utilizing a series of diblocks with almost constant total molecular weight; the aim is to identify the anchored chain configurational characteristics in the various regimes discussed above. In agreement with earlier studies [13], an interfacial partitioning of the block copolymer is observed at both the free surface and at the substrate interface. The investigation is performed with the  $^{15}\text{N}$  nuclear reaction analysis technique, which, in addition to the good resolution, makes it possible to use non deuterated block copolymers. No significant effect of the block length ratio on the total adsorbed amount was observed within the range of molecular weights investigated. The data are discussed in the framework of predictions based on adaptation of arguments from previous works [23–30] to the case of diblock copolymer adsorption. It is concluded that the systems investigated fall into the non-overlapping and the overlapping mushroom regimes whereas the brush regime was not accessible; however, no actual border between the two mushroom regimes can be identified with respect to the total adsorbed amount.

The rest of this article is arranged as follows: following the experimental Section 2, the results of the nuclear reaction analysis investigations are presented in Section 3

**Table 1.** Molecular characteristics of the polymers used.

Species	$M_w$	$M_w/M_n$	$w_{PS}^a$	$N^b$	$f_{PS}^c$
SI-20	162 000	1.05	0.198	2004	0.179
SI-30	150 000	1.06	0.295	1833	0.269
SI-36	142 000	1.06	0.359	1722	0.330
SI-57	159 000	1.05	0.573	1876	0.542
SI-68	133 000	1.05	0.678	1548	0.650
SI-76	153 000	1.06	0.760	1762	0.736
PSD	190 000	1.03	1.000	2125	1.000

<sup>a</sup>: Polystyrene weight fraction. <sup>b</sup>: Based on average segmental volume. <sup>c</sup>: Polystyrene volume fraction.

followed by discussion with respect to theory; concluding remarks are reserved for Section 4.

## 2 Experimental section

### 2.1 Materials and sample preparation

A series of poly(styrene-*block*-1,4 isoprene), SI, diblock copolymer samples were synthesized by anionic polymerization using a high vacuum-technique. The details of the synthesis and characterization have been described elsewhere [32–34]. First a small fraction of a prescribed amount of isoprene (I) monomer was reacted in *n*-heptane with *sec*-butyllithium for 20 min at 60 °C (a seeding reaction). Then the remaining monomer was introduced and allowed to polymerize at room temperature for 48 hr to obtain the precursor polyisoprenyl anions. Under these conditions, narrow molecular weight distribution highly-*cis*-polyisoprenes (PI) were obtained. Most of the solvent *n*-heptane was then replaced by benzene *via* vacuum distillation and a prescribed amount of styrene (S) monomer was introduced and allowed to react with the living macroanions. After 48 hr of reaction at room temperature the resulting SI anions were terminated with methanol to recover the block copolymer. The product was precipitated in methanol, dissolved in benzene again and freeze-dried and stored in vacuum until use. The synthetic procedure produced a polyisoprene (PI) sequence with a ratio of *cis*:*trans*:vinyl  $\approx 75:20:5$ . The characteristics of the diblocks are shown in Table 1. The deuterated polystyrene (PSD), which was used as the matrix homopolymer, was purchased from Polymer Standards Service (PSS) and used as received; its characteristics are also shown in Table 1.

For the nuclear reaction analysis measurements samples with a size of 19 mm  $\times$  38 mm were used. The films were prepared on silicon substrates of thickness 0.5 mm. In order to obtain a reproducible quality of the substrate surface the silicon wafers were treated in a mixture of hydrogen peroxide and ammonia (50 ml hydrogen peroxide 30%, 50 ml ammonia solution 25%, 100 ml nano-pure water) at 60 °C for 30 min and subsequently rinsed with nano-pure water.

The deuterated polystyrene and the block copolymer (15 wt% BCP) were dissolved in toluene at a concentration

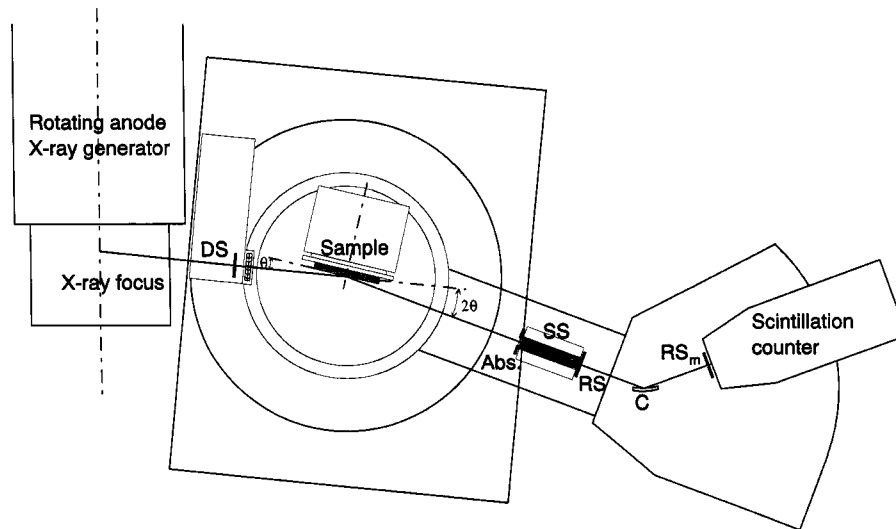


**Fig. 1.** The new X-ray reflectometer at FORTH-IESL in Heraklion: DS = divergence slit (width  $50\ \mu\text{m}$ ), abs. = absorber, SS = Soller slit (divergence angle  $0.34^\circ$ ), RS = receiving slit (width  $1.4\ \text{mm}$ ), C = curved graphite monochromator,  $\text{RS}_m$  = monochromator receiving slit.

of approximately  $20\ \text{mg}$  per ml solvent and stirred over night. The samples were prepared by the spin-coating technique. After preparation, the samples were annealed in a vacuum furnace at  $160\ ^\circ\text{C}$  for 24 hours. All the samples used were characterized by phase-measurement interference microscopy [35] and X-ray reflectivity.

## 2.2 X-ray Reflectometry

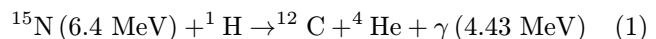
X-ray reflectivity measurements were performed with the new X-ray reflectometer at FORTH-IESL in Heraklion. It consists of a Rigaku 12 kW rotating anode X-ray generator and a Rigaku RINT 2000 Series wide angle diffractometer equipped with a Thin Film Attachment. A schematic drawing of the setup used is shown in Figure 1. The beam from the X-ray generator is collimated with the divergence slit DS ( $50\ \mu\text{m}$ , distance from focus  $10\ \text{cm}$ ) and impinges upon the sample surface, where it is partially reflected. After passing a Soller slit (divergence angle  $0.34^\circ$ ) and a graphite monochromator, the reflected beam is measured by a scintillation counter. For small angles of incidence, Al-attenuators are used in front of the Soller slit. On the back side of the Soller slit, a receiving slit RS (width  $1.4\ \text{mm}$ ) is used in order to suppress off-specular scattering from the sample. The goniometer radius (= distance sample-focus and sample-RS) is  $185\ \text{mm}$ . The divergence of the incident beam is  $0.027^\circ$  and reflectivities down to  $10^{-6}$  can be measured.

With these measurements, the total sample thickness and the surface roughness can be obtained [35]. The analysis is performed using a multilayer technique.

## 2.3 $^{15}\text{N}$ Nuclear reaction analysis

The concentration profile of the block copolymers is determined using the  $^{15}\text{N}$  nuclear reaction analysis

technique [36] as a direct depth profiling method with high resolution. The technique is based on the resonant reaction  $\text{H}(^{15}\text{N}, \alpha\gamma)^{12}\text{C}$



which occurs at a resonance energy  $E_r = 6.4\ \text{MeV}$ . The energy of the emitted  $\gamma$ -radiation is  $E_\gamma = 4.43\ \text{MeV}$ . If an ion beam with an energy  $E_B > E_r$  hits the sample, the ions lose energy as they penetrate into the film, and, at a certain depth, the resonant reaction with the hydrogen is possible. The depth scale is obtained from the energy loss  $dE/dx$ , that is specific for the material used (mainly polystyrene here). For samples containing deuterium, however, in addition to the reaction described above non-resonant reactions of the  $^{15}\text{N}$ -ion with the deuterium occur which give rise to a background of  $\gamma$ -radiation with energy in the range of  $E_\gamma$ . Figure 2 shows three different  $\gamma$ -spectra (the  $x$ -axis corresponds to the  $\gamma$ -radiation energy scale) for: (a) a film that contains no deuterium, where the radiation at  $4.43\ \text{MeV}$  is due to the  $^1\text{H}$  in the sample; (b) a film which contains both hydrogen and deuterium but when the energy of the incident ion beam is below  $E_r$ , and, therefore, the  $\text{H}(^{15}\text{N}, \alpha\gamma)^{12}\text{C}$  does not take place; (c) a film which contains both deuterium and hydrogen at ion beam energies higher than  $E_r$ . The background in case (c) is then eliminated assuming that the ratio of the background  $B$  and the integral  $R$  (Fig. 2c) is independent of the energy of the incident beam, so that it can be determined at beam energies below the resonance energy  $E_r$  in Figure 2b.

The measurements were performed with the new polymer measurement chamber at the Institut für Kernphysik, Universität Frankfurt. This chamber has the advantage that samples can be cooled with the vapor of liquid nitrogen down to  $-120^\circ$ , which makes it possible to investigate more radiation sensitive polymers than at room temperature. In addition a pressure of  $10^{-7}\ \text{mbar}$  can be obtained

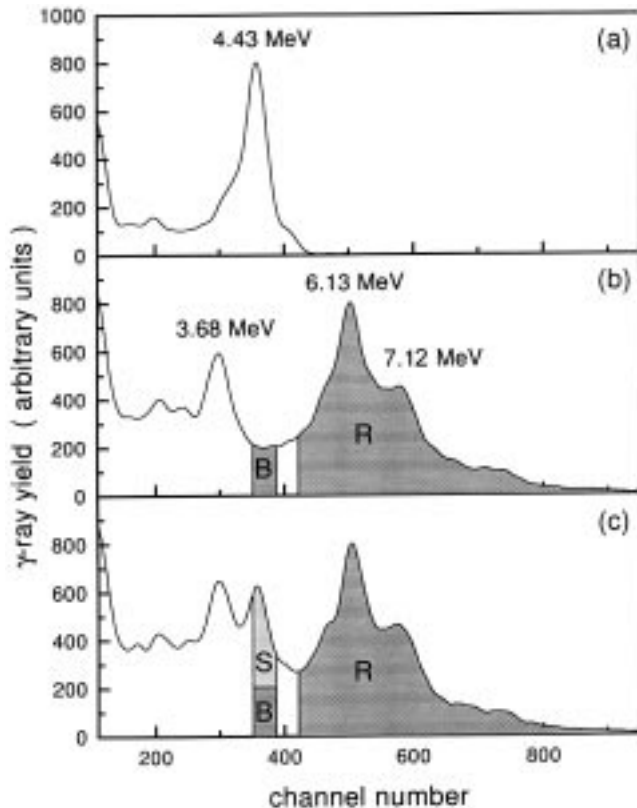


**Fig. 2.**  $\gamma$ -spectra of (a) a polymer film containing no deuterium and a film of partially deuterated polymer at an incident ion beam energies  $E_B$  lower (b) and higher (c) than the resonance energy  $E_r$ .

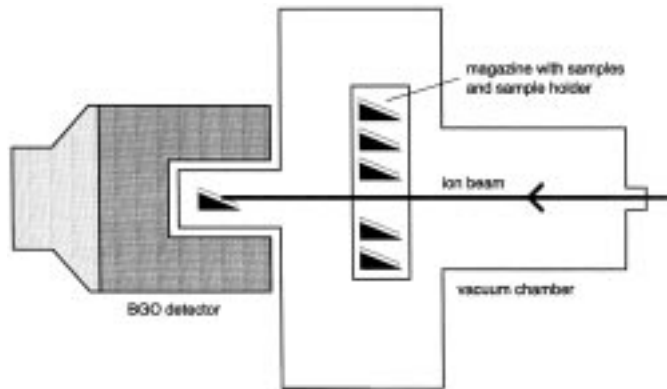


**Fig. 3.** Schematic drawing of the  $^{15}\text{N}$  sample and detection chamber.

in the chamber, which is pumped with a turbomolecular pump in connection with a rotary pump. The schematic drawing of the setup used is shown in Figure 3. A magazine inside the chamber can contain up to 12 samples, which are mounted on sample holders with a tilt-angle of  $9.4 \pm 0.1^\circ$ . With the help of a stepping motor this magazine can be moved vertically so that the sample holders can be pushed into a flange inside the hole of a 4 in  $\times$  4 inch BGO-detector. Because of this favorable geometry detection efficiencies of approximately 25% of the  $\gamma$ -rays

can be achieved [37]. The ion dose on the sample is determined using a tripod (three-pronged star) rotating in the ion-beam that is connected to a current integrator.

### 3 Results and discussion

After preparation by spin-coating all the samples were annealed in a vacuum oven at  $160^\circ$  for 24 hours in order to attain thermal equilibrium. To estimate whether this annealing time is sufficiently long for equilibrium one can use the equation for the diffusion in one direction  $\langle z^2 \rangle = 2Dt$  where  $\langle z^2 \rangle$  is the mean-squared displacement of a chain,  $D$  the diffusion coefficient and  $t$  the diffusion time. Using the film thickness  $d$  for  $\langle z^2 \rangle^{1/2}$  it is possible to get an estimate for the time  $t$  required to achieve equilibrium. Since the tracer diffusion coefficients of the SI block copolymers in the polystyrene melt are not known it is assumed that the self-diffusion coefficient of the matrix polystyrene (which has a slightly higher molecular weight) can be used instead. This was measured as [38]  $D = 0.007 M^{-2}$  at  $174^\circ\text{C}$  with  $D$  in  $\text{cm}^2/\text{s}$  and  $M$  in  $\text{g/mol}$ . Using the Williams-Landel-Ferry (WLF) equation [39] and the WLF coefficients for polystyrene [40] one can calculate the diffusion coefficient of polystyrene with a molecular weight of 190 000  $\text{g/mol}$  at  $160^\circ\text{C}$ ; using this value one obtains a time  $t = 37$  min for a diffusion path of 130 nm (a time of 26 min is estimated for a polystyrene of molecular weight 160 000 similar to that of the diblocks). Although the above assumption for the estimation of the copolymer diffusion coefficient is only very rough, the fact that the estimated time is 40 times less than the annealing time of 24 hours validates the assumption that the samples have already reached equilibrium. Besides, earlier studies [13] using a very high molecular weight asymmetric diblock ( $M_w = 1.08 \times 10^6$ , 99 wt% deuterated styrene) in a very high molecular weight polystyrene matrix ( $M_w = 3 \times 10^6$ ) showed that equilibrium was achieved within 1–2 days of annealing at  $190^\circ\text{C}$ . This also assures us that thermodynamic equilibrium was reached in the present case.

Following annealing, the samples were characterized with X-ray reflectometry in order to obtain the film thickness and the surface roughness. Figure 4 shows a typical reflectivity curve obtained from an annealed sample (in this case for a 15 wt% SI-57 / PSD film), where the Kiessig fringes observed are due to total film thickness oscillations. The solid line corresponds to the X-ray reflectivity curve calculated from a polystyrene film with thickness 116 nm and surface roughness of 0.34 nm. For all annealed samples the reflectivity measurements prove the existence of a nice film with surface roughness of the order or less than 0.5 nm, which is a typical value found for pure polystyrene samples prepared by spin-coating. The only exception is the sample with the highest polyisoprene content in the block copolymer (SI-20): for this sample, dewetting can be observed even by the naked eye, *i.e.* the sample looks rough. The X-ray reflectivity measurement for this 15 wt% SI-20/PSD film is shown in the inset of Figure 4; interference fringes with a much lower frequency (corresponding to a much smaller thickness) are

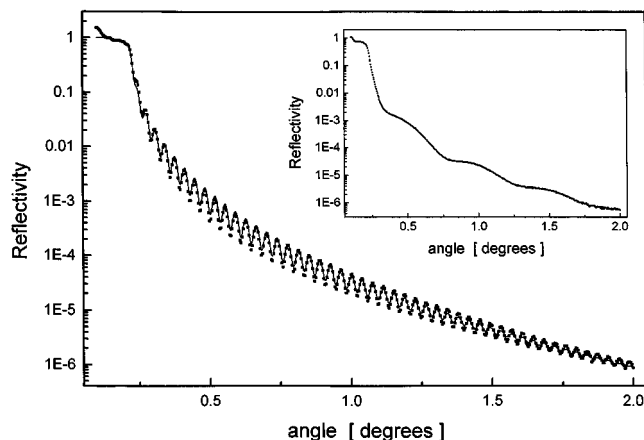


**Fig. 4.** X-ray reflectivity measurement of a 15 wt% SI-57/PSD sample on silicon after annealing. The solid line is the model calculation using a homogeneous polystyrene film with total thickness is 116 nm. Inset: X-ray reflectivity measurement of a 15 wt% SI-20/PSD sample on silicon after annealing. In this case, auto-dewetting takes place and the curve changes drastically; however, directly on the substrate one can still find a homogeneous film with a thickness of 8.7 nm.

observed. A thin polymer layer with a thickness of about 8.7 nm remains on the substrate on which auto-dewetting took place. Auto-dewetting has been observed before in the cases of polystyrene dewetting the free surface of an oriented symmetric poly(styrene-*b*-vinylpyridine) diblock copolymer thin film, which exposes a dense brush of the polystyrene to the air interface [41], as well as of end-functionalized polystyrene dewetting a thin film of the same material tethered to the substrate [42]; in both cases it was explained as being due to the lack of interpenetration of the polystyrene homopolymer with the dense brush formed either by the polystyrene block of the diblock [41] or by the densely packed tethered chains [42]. Also, auto-dewetting was observed when a polymer monolayer remained on the substrate following a pseudo-dewetting of either polystyrene [43] or a poly(ethylene oxide) [44] thin film on a silicon wafer; it was explained to be a consequence of conformational differences between adsorbed and non-adsorbed molecules.

For the nuclear reaction analysis measurements, the samples were cooled down to  $-100^{\circ}\text{C}$  in order to reduce the experimental error due to degradation of the polymer. In addition, the ion charge used for each data point was kept as low as possible. Since the samples contain much more deuterated polystyrene compared to the protonated block copolymer, a high background in the hydrogen window of the energy spectrum is present (see Fig. 2 and discussion in Sect. 2). This background is comparable to the signal from the block copolymer or even greater (within the sample the block copolymer concentration is quite small), and, therefore, one has to work very carefully in order to reduce the systematic error. All the  $\gamma$ -spectra measured were stored and after the measurements a correction for a slight electronic drift of the energy window was performed using the strong deuterium-peak at 6.13 MeV.

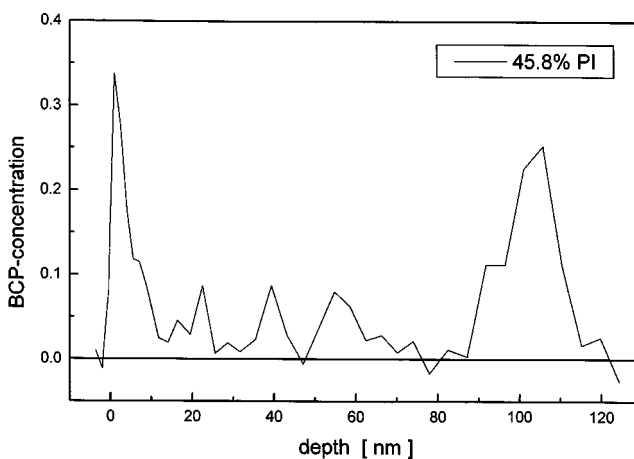


**Fig. 5.** Block copolymer concentration profile for the 15 wt% SI-57/PSD sample on silicon after annealing. Partitioning at both interfaces is evident.

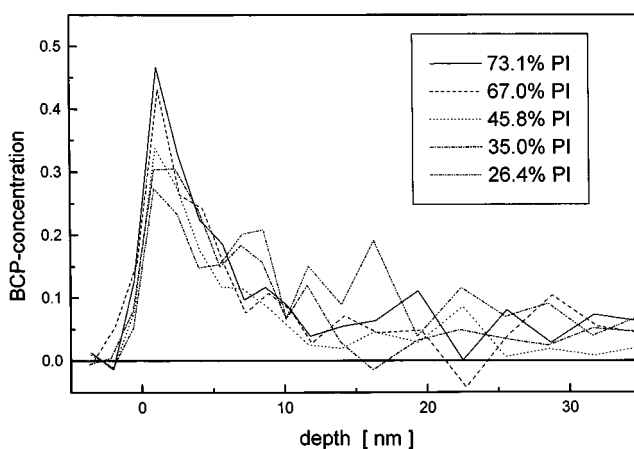


**Fig. 6.** Comparison of the concentration profiles near the air/polymer interface for the 15 wt% SI/PSD samples with block copolymers with different polyisoprene volume fractions.

The depth profiles are shown in Figures 5 and 6. In Figure 5, the depth profile for the entire film of the 15% SI57/PSD sample is shown ( $f_{PS} = 0.542$ ). One can clearly observe the surface enrichment at both the air/polymer and the polymer/substrate interfaces. To compare the relative enrichment at the two interfaces one has to keep in mind that the experimental resolution worsens with depth [35] leading to a stronger smearing at the polymer substrate interface; the resolution at the surface is about 3 nm compared to 10 nm at a depth of 100 nm. It is also evident that it is difficult to accurately determine the small block copolymer concentration in the middle of the film, since, for that part of the sample, the background due to the deuterium side reactions in the hydrogen energy window is a very significant fraction of the signal.

In Figure 6, the block copolymer profiles close to the air surface are compared for different samples; the good resolution of the technique at the top surface is evident. The width of the “interface” between the enrichment layer and the bulk of the sample, although not sharp,

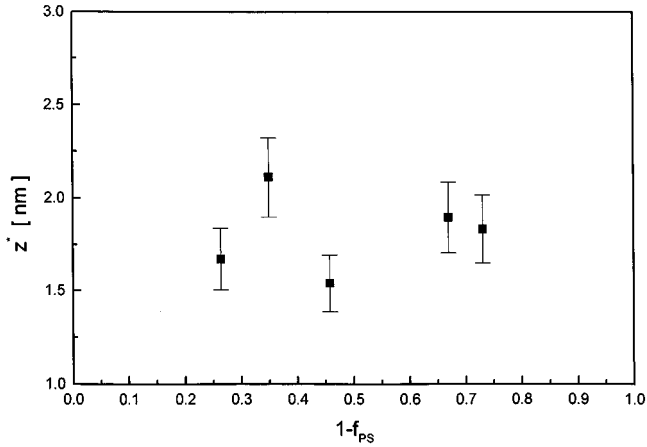


**Fig. 7.** The dependence of the surface excess  $z^*$  on block copolymer composition.

is comparable with the experimental resolution, and, therefore one cannot resolve the exact form of the profile and distinguish between different model fits. For all the samples shown, it is evident that the block copolymer concentration right at the surface decreases with increasing polystyrene fraction  $f_{PS}$ , whereas the thickness of the enrichment layer (of the order of 10 nm) apparently increases with  $f_{PS}$ . Due to the noise present in the data, it is difficult to quantify this increase in the thickness in order to estimate its scaling with the molecular weight of the polystyrene dangling block. Using the profiles in Figure 6, the surface excess can be calculated for each sample as:

$$z^* = \int_{interface} [\varphi(z) - \varphi_b] dz \quad (2)$$

where  $\varphi(z)$  is the copolymer concentration at depth  $z$  and  $\varphi_b$  is that away from the interface. This surface excess is shown *versus* the composition of the diblock copolymer in Figure 7. A very small variation of  $z^*$  on block copolymer composition is observed [45] whereas the values of the surface excess are comparable with but lower than the values reported by Budkowski *et al.* [13] for different molecular weights as a function of the concentration away from the surface. In our films, the concentrations away from the surface are in the range of 2.5–5% but they cannot be determined accurately. For this range of concentrations away from the surface Budkowski *et al.* show values ranging from  $\sim 2$  nm for  $10^4$ – $10^4$  SI copolymer to  $\sim 7$ – $12$  nm for a highly asymmetric  $10^6$ – $10^4$  SI diblock in a matrix of  $3 \times 10^6$  PS homopolymer. It should be noted that although the apparent layer thickness is of the order of the copolymer radius of gyration ( $\sim 10$  nm), the mean concentration at the interface, which is much less than one, results in  $z^*$  values around 2–2.5 nm. Note that a different normalization might result in different absolute values for  $z^*$ ; however the trend with copolymer composition will not be affected.

The effect of copolymer composition on the adsorbed amount and the layer thickness for the case of block

copolymer adsorbed onto a solid surface from solution in a solvent good for the dangling block has been studied by Evers *et al.* [4] in the framework of the self-consistent-field theory of Scheutjens and Fler. It was found that both the adsorbed amount and the layer thickness depend strongly on the chain composition. When the total length of the diblock copolymer was kept constant, a maximum was found in the total coverage as a function of the fraction of adsorbing segments; this behavior was also observed experimentally [10]. The maximum was found at a lower fraction of adsorbing segments with increasing chain length, bulk solution concentration, and surface affinity for the anchoring block. Reducing the surface affinity reduces the maximum value of the adsorbed amount, which can even disappear. Since, in the case of polymer melts, due to the small entropy of mixing even a small difference in surface tensions can result in a strong surface enrichment, this might be a reason for the absence of the dependence of the effect observed in our case. However, for polymer melts a detailed theoretical description is still needed.

Although there is a considerable amount of theoretical work on end-anchored homopolymers in the melt, the behavior of block copolymer adsorption at either a solid interface or a free surface has not been treated in detail. More specifically the effects of diblock composition on either the adsorbed amount or the segment density profile of the adsorbed layer have not been investigated. On the other hand emphasis was placed on the dependence of the adsorbed profile on the surface interactions and the bulk concentration for end-anchored homopolymers whereas the investigations were limited to the brush regime [26].

A qualitative description of the diblock composition dependence of the surface excess can be given within the framework of the theory of Alexander [31], de Gennes [23] and their extensions [24–30] in a similar way as was attempted for the block copolymer adsorption from solution [9]. The free-surface segregation is caused by the lower surface tension of the polyisoprene block. The polyisoprene acts as an anchor for the polystyrene block which dangles into the polystyrene homopolymer melt. Since the number of segments of the matrix homopolymer ( $P$ ) is, in the case investigated in the present work, larger than that of the dangling chain ( $N$ ) three limiting regimes can be envisioned depending on the mean distance  $s$  between anchoring points (as mentioned in the introduction): the non-overlapping mushroom regime for distances  $s$  larger than the size of the polystyrene-block coil in the bulk (when the conformation of the dangling polystyrene chain is ideal); the overlapping mushroom regime for intermediate  $s$  (when the mushrooms overlap but the polystyrene blocks are not stretched); the dry brush regime for very small  $s$  (when the polystyrene blocks are expected to be stretched and the matrix chains do not penetrate the brush).

For large fractions of the polyisoprene anchoring block, *i.e.* for small  $f_{PS}$ , it may be assumed that the system approaches the non-overlapping mushroom regime. In this case, the anchoring block can be thought of as forming a thin layer spread out as a “pancake” on the surface with

each polyisoprene block being confined inside a disc of diameter  $s$  and small, more or less constant, thickness of the order of a few segments. The volume of the disc (equal to  $N_{PI}v$ ,  $v$  being the segmental volume) is thus proportional to  $s^2a$ , where  $a$  is the segment length. The number of monomers of the anchoring block ( $N_{PI}$ ) should then be proportional to  $s^2$ . Thus,  $s \propto N_{PI}^{1/2}a$ , where it is assumed that  $v \approx a^3$ . This dependence of  $s$  on the molecular weight of the anchoring block has been experimentally verified for diblock copolymers adsorbed onto a solid surface from solution using a series of diblocks with constant molecular weight of the dangling block [9]. The dangling chain in this case can be considered as occupying a half-sphere with an ideal radius  $L \cong aN_{PS}^{1/2}$ , where  $N_{PS}$  is the length of the dangling block. The amount of block copolymer at the surface (the surface excess  $z^*$ ) is proportional to the surface density of anchored chains  $\sigma = s^{-2}$  times the number of segments of the block copolymer (note that experimentally both blocks of the copolymers are probed). Therefore:

$$z^* \propto \sigma N_{BCPV} \propto a N_{PI}^{-1} N_{BCP} \quad (3a)$$

or

$$z_{\text{non-overlapping mushroom}}^* \propto a(1 - f_{PS})^{-1}. \quad (3b)$$

Besides, the average volume fraction of the tethered chains inside the adsorbed layer should scale as  $\bar{\varphi} \cong N_{PS}v/(Ls^2) = N_{PS}^{1/2}\sigma a^2 \approx N_{BCP}^{-1/2}f_{PS}^{1/2}/(1 - f_{PS})$  and  $\bar{\varphi} < N_{PS}^{-1/2} \ll 1$ . Note that for grafted chains in a polymer melt, this limiting regime can be achieved [23,27–29] for grafting densities  $\sigma a^2 = s^{-2}a^2 < N_{PS}^{-1}$ , *i.e.* for polystyrene volume fractions  $f_{PS} < 0.5$ .

For small fractions of the polyisoprene block at the other limit, *i.e.* for large  $f_{PS}$ , one may approach the brush regime with overlapping stretched polystyrene chains. In this case and in the limit of high grafting densities [27] ( $\sigma a^2 > N^{-1/2}$  for  $P > N_{PS}$ ), the matrix chains are expected to be almost completely expelled [27–29] from the stretched brush (dry brush) with the brush thickness given by  $L \approx a^3 N_{PS} \sigma$ . Two main contributions to the free energy of the anchored copolymer chains on the surface should be considered: the gain in energy by the polyisoprene, PI, segments adsorbing to the surface; the combination of the repulsive elastic energy and the mixing energy. The adsorption energy represents [13] the sum of: the energy gained by the PI moiety by escaping from the unfavorable interactions with the PS host,  $N_{PI}\chi$  ( $\chi$  is the interaction parameter between PS and PI); the surface energy reduction gained by the lower surface tension of PI, which may be assumed to be proportional to the number of sticking monomers  $n = rN_{PI}$  ( $r$  is the fraction of PI monomers sticking to the surface) times the difference in surface energies per monomer  $\delta$ . For sufficiently large  $N_{PI}$ , both  $r$  and  $\delta$  should approach constant values independent of  $N_{PI}$ . Therefore,  $F_{\text{sticking}}/kT \cong (\chi N_{PI} + rN_{PI}\delta)$ . In this regime, the repulsive energy contribution is merely the elastic term calculated as [29]  $F_{\text{elastic}}/kT \cong N_{PS}(\sigma a^2)^2$ . The balance between the repulsive and the sticking energies results in

$\sigma \approx a^{-2} [\varepsilon N_{PI}/N_{PS}]^{1/2}$ , where  $\varepsilon = \chi + r\delta$ . The block copolymer surface excess is then,

$$z^* \propto \sigma N_{BCPV} \propto a \left[ \frac{\varepsilon N_{PI}}{N_{PS}} \right]^{1/2} N_{BCP} \quad (4a)$$

which leads to the limiting behavior

$$z_{\text{dry brush}}^* \propto \varepsilon^{1/2} \left[ \frac{1 - f_{PS}}{f_{PS}} \right]^{1/2} N_{BCP}. \quad (4b)$$

In this regime the average volume fraction of dangling chains inside the adsorbed layer  $\bar{\varphi} \cong O(1)$ . In this approach the influence of the small chemical difference between the deuterated dangling chains and the matrix hydrogenous homopolymer is not included [27] because, in the dry brush regime, the  $P$  chains are expected to be almost completely expelled from the brush. Moreover the equilibrium between the adsorbed chains and possible free diblock chains in the matrix is not taken into consideration (a detailed free energy calculation has been performed by Budkowski *et al.* [13]).

For intermediate  $\sigma$  values in the overlapping mushroom regime (it was also called non-stretched brush [28]), the repulsive interactions are not sufficient to swell the anchored chains and the conformation of the grafted chain remains Gaussian, *i.e.*  $L \approx aN_{PS}^{1/2}$ ; for  $P > N_{PS}$  this regime is attained for  $N_{PS}^{-1} < \sigma a^2 < N_{PS}^{-1/2}$ . In this regime the tethered chains behave as if they were isolated; there is no significant stretching and no penalty due to mixing with similar chains. Two different end-tethered chains overlap in this regime but the Flory approach shows that this does not lead to any difference in the free energy because of the screening. This means that from a free energy point of view essentially there is no real border between this regime and the non-overlapping mushroom regime [46]. Besides one cannot use arguments similar to those for the brush regime in order to estimate the dependence of the anchoring density (and thus of the adsorbed amount) on the copolymer block molecular weight. Therefore, the scaling of the adsorbed amount on diblock composition (Eq. (3)) should also more or less extend in the overlapping mushrooms regime. It is noted that the average volume fraction of the dangling chains inside the adsorbed layer is  $N_{PS}^{-1/2} < \bar{\varphi} < 1$ , *i.e.* larger than in the non-overlapping mushroom regime.

The dependence of the surface excess,  $z^*$ , on the composition of the diblock copolymer is thus given by equations (3, 4) for the limiting mushroom and dry brush regimes. It is the crossover between these different regimes which may potentially lead to a maximum of the surface excess  $z^*$  versus  $f_{PS}$ . However, the characteristics (height and position) of this maximum depend on the sticking energy parameter  $\varepsilon$  and on the molecular weights of the copolymer and the matrix. The maximum may thus be very shallow or outside the range of our experiments. For example, one can question whether the diblock copolymer systems investigated allow access to all the three regimes above. The fraction of the polyisoprene anchoring blocks

in our systems cover the range from 26% for SI-76 to 73% for SI-30 (since the SI-20 showed dewetting). According to the discussion above diblocks with  $f_{PS} < 0.5$  (*i.e.*, polyisoprene fraction larger than 0.5) should fall in the non-overlapping mushroom regime, whereas it is apparent that even the shorter polyisoprene block (26%) is not short enough to allow the brush conformation (for the behavior in solution see Refs. [8,9]). Therefore, our systems apparently span the non-overlapping mushrooms and the overlapping mushrooms regimes without the data allowing identification of any clear border in between. Note, however, that the data do not even follow equation (3) for the mushroom regime.

#### 4 Concluding remarks

Using the  $^{15}\text{N}$  nuclear reaction analysis technique the surface segregation of poly(styrene-block-1,4 isoprene) diblock copolymers has been investigated in thin films of polystyrene/diblock mixtures; the concentration profiles of the block copolymers were measured in a matrix of deuterated polystyrene. A segregation of the diblock copolymer was found at the free surface as well as at the polymer/substrate interface. The quality of the samples measured was characterized by X-ray reflectometry and it was found that the surface roughness was comparable to a homopolymer polystyrene film. The only exception was the film with the highest polyisoprene content where auto-dewetting was observed. For a series of copolymers with almost constant total molecular weight the surface excess was determined as a function of chain composition. A very weak (if any) dependence of the surface excess was observed on the diblock composition. The results were discussed on the basis of Flory-type arguments for the dependence of the adsorbed amount on block length ratio. Relevant parameters like the sticking energy  $\varepsilon$  are, however, not known and a more detailed theoretical model for the melt case is needed.

Currently, this work is being extended by investigating the detailed segment density profiles of the dangling chain of diblock copolymers adsorbed from the melt using neutron reflectivity and utilizing a series of diblocks with the same molecular weight of the dangling chain and different molecular weights of the anchoring block; the results will be reported elsewhere.

The authors thank Prof. K. Adachi for kindly supplying the diblock copolymer samples used in the present study. S.H. A. acknowledges that part of this research was sponsored by NATO's Scientific Affairs Division in the framework of the Science for Stability Programme and by the Greek General Secretariat of Research and Technology. K. K., S.H. A., and M. S. acknowledge the support from the European Union within the Programmes of International Scientific Cooperation (Contract ISC\*CT93-0951) and Human Capital and Mobility (Contract CHRX-CT93-0370). M. S. and F. R. greatly acknowledge the support by DFG and the technical help of M. Bach during the set-up of the nuclear reaction analysis apparatus. S.H. A. thanks Prof. I. Bitsanis for valuable discussions and

Dr. M. Aubouy for communicating his thoughts for the intermediate regime.

#### References

1. S.T. Milner, *Science* **251**, 905 (1991); A. Halperin, M. Tirrell, T.P. Lodge, *Adv. Pol. Sci.* **100**, 31 (1992).
2. I. Szleifer, M.A. Carignano, *Adv. Chem. Phys.* **94**, 165 (1996); I. Szleifer, *Current Opinion in Colloid Interf. Sci.* **1**, 416 (1996).
3. C. Marques, J.F. Joanny, L. Leibler, *Macromol.* **21**, 1051 (1988); C. Marques, J.F. Joanny, *Macromol.* **22**, 1458 (1989).
4. O.A. Evers, J.M.H.M. Scheutjens, G.H. Fler, *Macromol.* **25**, 5221 (1990); O.A. Evers, J.M.H.M. Scheutjens, G.H. Fler, *J. Chem. Soc. Faraday Trans.* **86**, 1333 (1990).
5. G. Hadziioannou, S. Patel, S. Granick, M. Tirrell, *J. Amer. Chem. Soc.* **108**, 2896 (1986); H.J. Taunton, C. Toprakcioglu, L.J. Fetters, J. Klein, *Macromol.* **21**, 3333 (1988).
6. H. Motschmann, M. Stamm, C. Toprakcioglu, *Macromol.* **24**, 3681 (1991); J.R. Dorgan, M. Stamm, C. Toprakcioglu, R. Jérôme, L.J. Fetters, *Macromol.* **26**, 5321 (1993).
7. S.K. Satija, C.F. Majkrzak, T.P. Russell, S.K. Sinha, E.B. Sirota, G.J. Hughes, *Macromol.* **23**, 3860 (1990).
8. J.B. Field, C. Toprakcioglu, R.C. Ball, H.B. Stanley, L. Dai, W. Barford, J. Penfold, G. Smith, W. Hamilton, *Macromol.* **25**, 434 (1992).
9. J.B. Field, C. Toprakcioglu, L. Dai, G. Hadziioannou, G. Smith, W. Hamilton, *J. Phys. II France* **2**, 2221 (1992).
10. D.A. Guzonas, D. Boils, C.P. Tripp, M.L. Hair, *Macromol.* **25**, 2434 (1992).
11. V.S. Wakharkar, T.P. Russell, V.R. Deline, in *Polymer Based Molecular Composites*, edited by D.W. Schaefer, J.E. Mark, *MRS Symposium Proceedings* **171**, 343 (1990).
12. P.F. Green, T.P. Russell, *Macromol.* **25**, 783 (1992).
13. A. Budkowski, U. Steiner, J. Klein, L.J. Fetters, *Europhys. Lett.* **20**, 499 (1992); A. Budkowski, J. Klein, U. Steiner, L.J. Fetters, *Macromol.* **26**, 2470 (1993); A. Budkowski, J. Klein, L.J. Fetters, *Macromol.* **28**, 8571 (1995); A. Budkowski, J. Klein, L.J. Fetters, T. Hashimoto, *Macromol.* **28**, 8579 (1995); J. Rysz, A. Bernasik, H. Ermer, A. Budkowski, R. Brenn, T. Hashimoto, J. Jedlinski, *Europhys. Lett.* **40**, 503 (1997).
14. F.J. Esselink, A.N. Semenov, G. ten Brinke, G. Hadziioannou, G.T. Oostergetel, *Phys. Rev. B* **46**, 13451 (1993).
15. T.P. Russell, S.H. Anastasiadis, A. Menelle, G.P. Felcher, S.K. Satija, *Macromol.* **24**, 1575 (1990).
16. K.R. Shull, E.J. Kramer, G. Hadziioannou, W. Tang, *Macromol.* **23**, 4780 (1990).
17. K.R. Shull, K.I. Winey, E.L. Thomas, E.J. Kramer, *Macromol.* **24**, 2748 (1991).
18. P.F. Green, T.P. Russell, *Macromol.* **24**, 2931 (1991).
19. K.H. Dai, E.J. Kramer, K.R. Shull, *Macromol.* **25**, 220 (1992).
20. X. Zhao, W. Zhao, M.H. Rafailovich, J. Sokolov, T.P. Russell, S. Kumar, S.A. Schwarz, B.J. Wiekens, *Europhys. Lett.* **15**, 725 (1991).
21. R.A.L. Jones, L.J. Norton, K.R. Shull, E.J. Kramer, G.P. Felcher, A. Karim, L.J. Fetters, *Macromol.* **25**, 2359 (1992).
22. C.J. Clarke, R.A.L. Jones, J.L. Edwards, K.R. Shull, J. Penfold, *Macromol.* **28**, 2042 (1995).



23. P.G. de Gennes, *Macromol.* **13**, 1069 (1980); P.G. de Gennes, *Adv. Colloid Interf. Sci.* **27**, 189 (1987).
24. L. Leibler, *Makromol. Chem., Macromol. Symp.* **16**, 1 (1988).
25. E.B. Zhulina, O.V. Borisov, *J. Colloid Interf. Sci.* **144**, 507 (1990).
26. K.R. Shull, *J. Chem. Phys.* **94**, 5723 (1991); K.R. Shull, *Macromol.* **29**, 2659 (1996).
27. M. Aubouy, E. Raphaël, *J. Phys. II France* **3**, 443 (1993).
28. E. Raphaël, P. Pincus, G.H. Fredrickson, *Macromol.* **26**, 1996 (1993).
29. M. Aubouy, G.H. Fredrickson, P. Pincus, E. Raphaël, *Macromol.* **28**, 2979 (1995).
30. C. Gay, *Macromol.* **30**, 5939 (1997).
31. S. Alexander, *J. Phys. France* **38**, 983 (1977).
32. M.-L. Yao, H. Watanabe, K. Adachi, T. Kotaka, *Macromol.* **25**, 1699 (1992); M.-L. Yao, H. Watanabe, K. Adachi, T. Kotaka, *Macromol.* **24**, 2955 (1991).
33. T. Jian, S.H. Anastasiadis, G. Fytas, K. Adachi, T. Kotaka, *Macromol.* **26**, 4706 (1993).
34. S.H. Anastasiadis, K. Chrissopoulou, G. Fytas, M. Appel, G. Fleischer, K. Adachi, Y. Gallot, *Acta Polym.* **47**, 250 (1996).
35. M. Stamm, *Adv. Pol. Sci.* **100**, 357 (1992).
36. D. Endisch, F. Rauch, A. Götzelmann, G. Reiter, M. Stamm, *Nucl. Instr. and Meth. B* **62**, 513 (1992).
37. T. Schurrat, Diploma thesis, Universität Frankfurt, 1996.
38. P.F. Green, C.J. Palmstrom, J.W. Mayer, E.J. Kramer, *Macromol.* **18**, 501 (1985).
39. J.D. Ferry, *Viscoelastic Properties of Polymers* (John Wiley & Sons, Inc., New York, NY, 1980).
40. A.J. Barlow, A. Erginsay, J. Lamb, *Proc. Royal Soc.* **A298**, 481 (1967).
41. Y. Liu, M.H. Rafailovich, J. Sokolov, S.A. Schwarz, X. Zhong, A. Eisenberg, E.J. Kramer, B.B. Sauer, S. Satija, *Phys. Rev. Lett.* **73**, 440 (1994).
42. G. Henn, D.G. Bucknall, M. Stamm, P. Vanhoorne, R. Jérôme, *Macromol.* **29**, 4305 (1996).
43. P.K. Müller-Buschbaum, P. Vanhoorne, V.K. Scheumann, M.K. Stamm, *Europhys. Lett.* **40**, 655 (1997).
44. G. Reiter, J.-U. Sommer, *Phys. Rev. Lett.* **80**, 3771 (1998).
45. The sample with the highest polyisoprene fraction in the copolymer (SI-20) shows an apparent surface enrichment ( $z^* \cong 4.1$  nm) which is much higher than in any other film. However, in that case auto-dewetting occurred and both the surface of the dewetting structure as well as the surface of the thin remaining film are observed; therefore, one should not compare this measurement to the others. This, however, indicates that the dewetting may take place on top of a brush formed by the copolymer segregation to the substrate interface.
46. M. Aubouy, private communication.